Annals of Biomedical Engineering, Vol. 37, No. 4, April 2009 (© 2009) pp. 824–838
DOI: 10.1007/s10439-009-9635-z

Evaluation of Stochastic Differential Equation Approximation of Ion Channel Gating Models

IAN C. BRUCE

Department of Electrical and Computer Engineering, Room ITB-A213, McMaster University, 1280 Main Street West, Hamilton, ON L8S 4K1, Canada

(*Received 10 September 2008; accepted 5 January 2009; published online 17 January 2009*)

Abstract—Fox and Lu derived an algorithm based on stochastic differential equations for approximating the kinetics of ion channel gating that is simpler and faster than "exact" algorithms for simulating Markov process models of channel gating. However, the approximation may not be sufficiently accurate to predict statistics of action potential generation in some cases. The objective of this study was to develop a framework for analyzing the inaccuracies and determining their origin. Simulations of a patch of membrane with voltage-gated sodium and potassium channels were performed using an exact algorithm for the kinetics of channel gating and the approximate algorithm of Fox & Lu. The Fox & Lu algorithm assumes that channel gating particle dynamics have a stochastic term that is uncorrelated, zero-mean Gaussian noise, whereas the results of this study demonstrate that in many cases the stochastic term in the Fox & Lu algorithm should be correlated and non-Gaussian noise with a non-zero mean. The results indicate that: (i) the source of the inaccuracy is that the Fox & Lu algorithm does not adequately describe the combined behavior of the multiple activation particles in each sodium and potassium channel, and (ii) the accuracy does *not* improve with increasing numbers of channels.

Keywords—Hodgkin–Huxley model, Biophysical model, Markov process, Activation particles, Inactivation particles, Membrane noise.

INTRODUCTION

The stochastic nature of voltage-dependent ion channel gating is thought to be functionally significant for a number of different types of neurons,[46] for cardiac myocytes,[20,21,41] and for pancreatic β cells.[10] One case that has received particular attention is electrical stimulation of auditory nerve fibers by an auditory prosthesis, or *cochlear implant*. The nodes of Ranvier in auditory nerve fibers are very small, such that they have relatively small numbers of ion channels, and consequently the physiological effects of stochastic ion channel gating are quite noticeable.[4,6,22–24,28–30] Furthermore, auditory nerve fibers typically do not receive synaptic input from a deaf ear implanted with an auditory prosthesis, and subsequently stochastic ion channel gating is likely to be the primary noise source in the neural response.[29] This view is supported by evidence that the physiological noise from ion channel gating has strong perceptual significance for cochlear implants users.[5,11,17,18]

The importance of ion channel gating statistics for cases such as neural stimulation by cochlear implants motivates the development of accurate and computationally efficient stochastic models of ion channel gating. Mino *et al.*[25] compared four different algorithms for implementing Hodgkin–Huxley models[16] with stochastic sodium channels: Rubinstein,[28] Strassberg and DeFelice,[40] Chow and White,[9] and Fox and Lu.[12,13] The first three algorithms utilize exact methods for describing channel kinetics with finite-state Markov process models. In contrast, the algorithm of Fox & Lu uses stochastic differential equations (SDEs) to approximate the Markov process models. In addition to being simpler, the approximate method of Fox & Lu is around seven times faster than the Chow & White algorithm, the fastest of the exact methods.[25] Consequently, the Fox & Lu algorithm has been widely used in the literature.[7,8,10,14,15,19,26,27,31–39,45,47–49]

However, for simulations of a patch of membrane with 1000 sodium channels, Mino *et al.*[25] reported that the approximate method of Fox & Lu produced quite different action potential (AP) statistics than the other methods. They consequently argued that, in spite of its computational advantage, the Fox & Lu algorithm may be too inaccurate in some circumstances to use reliably as an approximation to the exact methods. Further analysis by Bruce[2] showed that some of the inaccuracies described in Mino *et al.*[25] were due to the

Address correspondence to Ian C. Bruce, Department of Electrical and Computer Engineering, Room ITB-A213, McMaster University, 1280 Main Street West, Hamilton, ON L8S 4K1, Canada. Electronic mail: ibruce@ieee.org

method used in that study to determine the number of open sodium channels in the Fox & Lu algorithm. Mino *et al.*[25] rounded down the number of open sodium channels to an integer value, whereas Bruce[2] showed that more accurate results are obtained if the number of open sodium channels is rounded to the nearest integer. However, several important inaccuracies remained, which appear to result from incorrect relative noise levels in the Fox & Lu model.[2]

In this paper, a framework is introduced for analyzing the inaccuracies of the Fox & Lu algorithm and determining their source (preliminary results were presented in Bruce[1] and Bruce and Dinath[3]). In the Methods section, Markov process models of stochastic ion channel gating and Fox & Lu's SDE approximation are reviewed. Next, the methodology for analyzing the inaccuracies of the Fox & Lu algorithm is described. Finally, details are given of the simulations performed in this study. In the Results section, analyses of simulation results are compared with the theory of Fox and Lu[12,13] to determine the scope and the cause of the approximation's inaccuracies. In the Discussion section, the implications of the results for neural modeling are highlighted and directions for future research are suggested.

METHODS

Ion Channel Gating Models and Algorithms

The Hodgkin–Huxley model sodium channel has three independent activation particles m and one inactivation particle h, while the model potassium channel has four independent activation particles n.[16] The Markov kinetics for gating of sodium and potassium channels are given by

$$\begin{array}{ccccccc} m_0h_0 & \underset{\beta_m}{\overset{3\alpha_m}{\rightleftharpoons}} & m_1h_0 & \underset{2\beta_m}{\overset{2\alpha_m}{\rightleftharpoons}} & m_2h_0 & \underset{3\beta_m}{\overset{\alpha_m}{\rightleftharpoons}} & m_3h_0 \\ \alpha_h\downarrow\uparrow\beta_h & & \alpha_h\downarrow\uparrow\beta_h & & \alpha_h\downarrow\uparrow\beta_h & & \alpha_h\downarrow\uparrow\beta_h \\ m_0h_1 & \underset{\beta_m}{\overset{3\alpha_m}{\rightleftharpoons}} & m_1h_1 & \underset{2\beta_m}{\overset{2\alpha_m}{\rightleftharpoons}} & m_2h_1 & \underset{3\beta_m}{\overset{\alpha_m}{\rightleftharpoons}} & m_3h_1 \end{array} \quad (1)$$

and

$$n_0 \underset{\beta_n}{\overset{4\alpha_n}{\rightleftharpoons}} n_1 \underset{2\beta_n}{\overset{3\alpha_n}{\rightleftharpoons}} n_2 \underset{3\beta_n}{\overset{2\alpha_n}{\rightleftharpoons}} n_3 \underset{4\beta_n}{\overset{\alpha_n}{\rightleftharpoons}} n_4, \quad (2)$$

respectively, where α_x is the average rate of opening of particles of type x, β_x is the average rate of closing of particles of type x, and x_i indicates that i particles of type x are presently open in a particular channel.

If N_y indicates the number of channels currently in state y, then the number of open sodium and potassium channels in a patch of membrane is given, respectively, by

$$N_{\mathrm{Na}}(t) = N_{m_3h_1}(t) \quad (3)$$

and

$$N_{\mathrm{K}}(t) = N_{n_4}(t). \quad (4)$$

There are several different numerical techniques for simulating the Markov kinetics. Rubinstein[28] and Strassberg and DeFelice[40] utilize methods that keep track of the gating particle states of every ion channel, whereas the algorithm of Chow and White[9] takes the more efficient approach of just keeping track of the number of channels in each state.

Fox and Lu[12,13] showed that a master equation (cellular automaton) describing the Markov process for channel gating can be contracted to a Langevin description (via a Fokker–Planck equation). In Fox & Lu's algorithm, the dynamics of the fraction of open gating particles x is approximated by the SDE

$$\frac{dx(t)}{dt} = \alpha_x(t)(1 - x(t)) - \beta_x(t)x(t) + \tilde{g}_x(t), \quad (5)$$

where $x = m$, h, or n, the transition rates $\alpha_x(t)$ and $\beta_x(t)$ are instantaneous functions of the membrane potential $V(t)$, and the noise term $\tilde{g}_x(t)$ is Gaussian with moments

$$\langle \tilde{g}_x(t) \rangle = 0 \quad (6)$$

and

$$\langle \tilde{g}_x(t)\tilde{g}_x(t') \rangle = \frac{2}{N_{\mathrm{X}}^{\max}} \frac{\alpha_x(t)(1 - x(t))\beta_x(t)x(t)}{2} \delta(t - t'), \quad (7)$$

where X = Na for $x = m$ or h, X = K for $x = n$, and $N_{\mathrm{X}}^{\max}$ is the total number of ion channels of type X.

Note that Eq. (5) is equivalent to the deterministic Hodgkin–Huxley ordinary differential equation (ODE) for gating particle dynamics[16] but with the stochastic term $\tilde{g}_x(t)$ added.

Fox and Lu[12,13] showed that the noise term's 2nd moment (Eq. 7) can be approximated by

$$\langle \tilde{g}_x(t)\tilde{g}_x(t') \rangle = \frac{2}{N_{\mathrm{X}}^{\max}} \frac{\alpha_x(t)\beta_x(t)}{\alpha_x(t) + \beta_x(t)} \delta(t - t'). \quad (8)$$

In the Fox & Lu algorithm, the number of open sodium and potassium channels is estimated to be

$$N_{\mathrm{Na}}(t) = N_{\mathrm{Na}}^{\max} m^3(t)h(t) \quad (9)$$

and

$$N_{\mathrm{K}}(t) = N_{\mathrm{K}}^{\max} n^4(t), \quad (10)$$

respectively, where $N_{\mathrm{Na}}^{\max}$ and $N_{\mathrm{K}}^{\max}$ are the total number of sodium and potassium channels, respectively, in the patch of membrane.

Numerical solution of Eq. (5) can be achieved by applying Euler's method to obtain the discrete-time difference equation (e.g., see Eq. 5 of Tuckwell and Lansky[43])

$$x[k+1] = x[k] + \{\alpha_x[k](1 - x[k]) - \beta_x[k]x[k]\}\Delta t + \tilde{g}_x[k]\sqrt{\Delta t}, \quad (11)$$

where k is the sample number, Δt is the time step and $\tilde{g}_x[k]$ is a pseudorandom number with the statistics of $\tilde{g}_x(t)$.

Analysis of Open Channel Statistics

Fox and Lu[12,13] did not derive an analytical expression for the error in their approximation. In this paper, empirical analysis of simulation results is used to evaluate the accuracy of the Fox & Lu algorithm. It is impractical to conduct a complete analysis of the open channel probability distributions; even the mean and standard deviation in the number of open channels depend on the time courses of the values of the gating particle transition rates (i.e., the αs and βs in the preceding equations), which can vary in an infinite number of ways. However, an analysis of the open channel mean and standard deviations as a function of time for an "exact" algorithm and the Fox & Lu approximation in response to a voltage step proves to be both informative and practical.

The results of such an analysis (see Fig. 2) indicate that the change in the *mean* number of open channels for an exact Markov process algorithm as a function of time in response to a voltage step is well approximated by the Fox & Lu algorithm *but the standard deviation is not*. That is, the basic framework of the Fox & Lu algorithm—adding a noise term to the deterministic ODE of Hodgkin and Huxley—is consistent with the behavior of the Markov process algorithms, but the expressions for the noise term statistics derived by Fox & Lu may not be accurate in certain circumstances. Consequently, a methodology is developed next for analyzing simulations of a Markov process model and determining the equivalent noise term statistics for each gating particle under the Fox & Lu framework.

Methodology for Estimating an Equivalent Fox & Lu Noise Term from an "Exact" Algorithm

Presented here is an empirical method for estimating the *required* Fox & Lu noise term to match the channel gating statistics described by one of the "exact" models of the Markov kinetics.[9,28,40]

The first step in the process is to determine the gating particle values m, h, and n that would be required for the Fox & Lu algorithm to have the same number of open ion channels (according to Eqs. 9 and 10) as one of the exact methods (according to Eqs. 3 and 4) at each simulation time step. These estimated gating particle values will be referred to as $\hat{m}$, $\hat{h}$, and $\hat{n}$, respectively.

The second step is to determine what value the Fox & Lu noise terms (see Eq. 11) would have to take at each time step to explain the time series for $\hat{m}$, $\hat{h}$, and $\hat{n}$. The corresponding noise terms per time step will be referred to as $\Delta\hat{g}_m[k]$, $\Delta\hat{g}_h[k]$, and $\Delta\hat{g}_n[k]$.

Applying the first step of this methodology to the potassium channel is straightforward, because the number of open potassium channels in the exact methods and the Fox & Lu algorithm depends on only one random variable each, N_{n_4} and n, respectively. Equating Eqs. (10) and (4) gives that the n-particle value in the Fox & Lu algorithm would need to be exactly

$$\hat{n} = \sqrt[4]{\frac{N_{n_4}}{N_{\mathrm{K}}^{\max}}} \quad (12)$$

at each time step in order for the Fox & Lu algorithm to have the same number of open potassium channels as an exact method.

Such an exact relationship cannot be derived for the sodium channel, because the number of open sodium channels depends on a single random variable $N_{m_3h_1}$ in the exact methods (Eq. 3), whereas the Fox & Lu algorithm has two random variables, m and h, that determine the number of open sodium channels (Eq. 9). However, because of the independence of the sodium activation and inactivation transitions in the Markov process (Eq. 1), the fraction of sodium channels in the state $N_{m_3h_1}$ at each time step of an exact-method simulation is well estimated by the product $\hat{m}^3\hat{h}$, where the m-particle value is determined by the number of channels with three open m particles (irrespective of the h-particle states), i.e.,

$$\hat{m} = \sqrt[3]{\frac{N_{m_3h_0} + N_{m_3h_1}}{N_{\mathrm{Na}}^{\max}}}, \quad (13)$$

and the h-particle value is determined by the fraction of open h particles (irrespective of the m-particle states), i.e.,

$$\hat{h} = \frac{N_{m_0h_1} + N_{m_1h_1} + N_{m_2h_1} + N_{m_3h_1}}{N_{\mathrm{Na}}^{\max}}. \quad (14)$$

The second step, obtaining the noise terms from each of the estimated gating particle time series, is identical for each particle. From Eq. (11), the Fox & Lu noise term that would be required to track the

gating particle value $\hat{x}$ at each time step k computed from simulations using an exact method is

$$\Delta\hat{g}_x[k] = \hat{x}[k+1] - \hat{x}[k] - \{\alpha_x[k](1-\hat{x}[k]) - \beta_x[k]\hat{x}[k]\}\Delta t, \quad (15)$$

where $\hat{x} = \hat{m}$, $\hat{h}$, or $\hat{n}$.

By comparing the statics of $\Delta\hat{g}_m[k]$, $\Delta\hat{g}_h[k]$, and $\Delta\hat{g}_n[k]$ computed using Eq. (15) to the statistics of the analytical noise terms used in Eq. (11), i.e., $\tilde{g}_m[k]\sqrt{\Delta t}$, $\tilde{g}_h[k]\sqrt{\Delta t}$, and $\tilde{g}_n[k]\sqrt{\Delta t}$, a quantitative measure of the Fox & Lu approximation's accuracy is obtained. Note that the effect of the time step Δt is contained within each estimated noise term $\Delta\hat{g}_x[k]$. It is not possible to separate out the effect of the time step in the estimated noise term (as is done in Fox and Lu's derivation), because no assumptions are made *a priori* in this empirical method about the statistics of the estimated noise term.

Analysis of Action Potential Statistics

The analysis here is an extension of the simulations from Mino *et al.*[25] and Bruce[2] but with the number of sodium channels varied from 100 to 10,000. In those studies, several different metrics were utilized to quantify AP statistics. The firing efficiency (FE) is defined as the fraction of trials in which a stimulus elicits an AP, i.e., it is an estimate of the discharge probability. For trials in which an AP was generated, the mean and standard deviation of the spike latency were also calculated.

In this paper, the analysis of AP statistics is focused on how FE varies as a function of the current amplitude I for a single 100-μs monophasic depolarizing current pulse. Examples of FE vs. I curves are given by the symbols in Fig. 10. Following Verveen and Derksen,[44] these curves were fit by an integrated Gaussian function (solid lines in Fig. 10):

$$\mathrm{FE} = \frac{1}{2}\left(\mathrm{erf}\left(\frac{I - I_{\mathrm{th}}}{\sqrt{2}\sigma}\right) + 1\right), \quad (16)$$

where I_{th} is the mean threshold current (i.e., corresponding to a FE of 50%) and σ is the standard deviation in threshold fluctuations.[44]

The relative noise level can be quantified by the *relative spread* (RS), the standard deviation in threshold fluctuations normalized by the mean threshold current,[44] i.e.,

$$\mathrm{RS} = \frac{\sigma}{I_{\mathrm{th}}}. \quad (17)$$

Simulations

To understand how the channel gating statistics affect the auditory nerve fiber AP statistics investigated in Mino *et al.*[25] and Bruce,[2] simulations are performed using the equations utilized in those studies for the sodium transition rates. In addition, simulations are performed using equations for the potassium transition rates that are also appropriate for the node of Ranvier in auditory nerve fibers.[24]

Following Mino *et al.*,[24,25] the activation and inactivation particle transition rates vary with the relative transmembrane potential V according to

$$\alpha_m = \frac{1.872(V - 25.41)}{1 - \mathrm{e}^{(25.41-V)/6.06}} \quad (18)$$

$$\beta_m = \frac{3.973(21.001 - V)}{1 - \mathrm{e}^{(V-21.001)/9.41}} \quad (19)$$

$$\alpha_h = \frac{-0.549(27.74 + V)}{1 - \mathrm{e}^{(V+27.74)/9.06}} \quad (20)$$

$$\beta_h = \frac{22.57}{1 - \mathrm{e}^{(56.0-V)/12.5}} \quad (21)$$

$$\alpha_n = \frac{0.129(V - 35)}{1 - \mathrm{e}^{(35-V)/10}} \quad (22)$$

$$\beta_n = \frac{0.3236(35 - V)}{1 - \mathrm{e}^{(V-35)/10}}, \quad (23)$$

where the rates have units of ms^{-1} and V has units of mV.

For the analysis of open channel statistics, voltage clamp experiments with a voltage step were simulated. Specifically, the holding potential (V_h) was the resting potential ($V = 0$), and the membrane potential was stepped to a value of V_c at $t = 0.1$ ms, as shown in the bottom panel of Fig. 1. For these simulations, the patch of membrane had 1000 sodium and 333 potassium channels. The mean and standard deviation of the number of open channels at each time step (according to Eqs. 3 and 4 for an "exact" algorithm and Eqs. 9 and 10 for the Fox & Lu algorithm) were calculated for 1000 repetitions of each voltage step. A sampling step Δt of 1 μs was utilized.

Equation (8) indicates that the dominant factor in the Fox & Lu noise term statistics is the present values of the transition rates, which in turn depend only on the present value of the relative transmembrane potential (see Eqs. 18–23). Therefore the simulations to analyze the noise-term statistics were run in voltage clamp condition with a constant relative transmembrane potential. Because the holding potential was identical to the clamp potential in these simulations, the potential is just referred to as V, the relative transmembrane potential.

Voltage clamp simulations were performed with a sampling step Δt of 1 μs. The simulated duration for

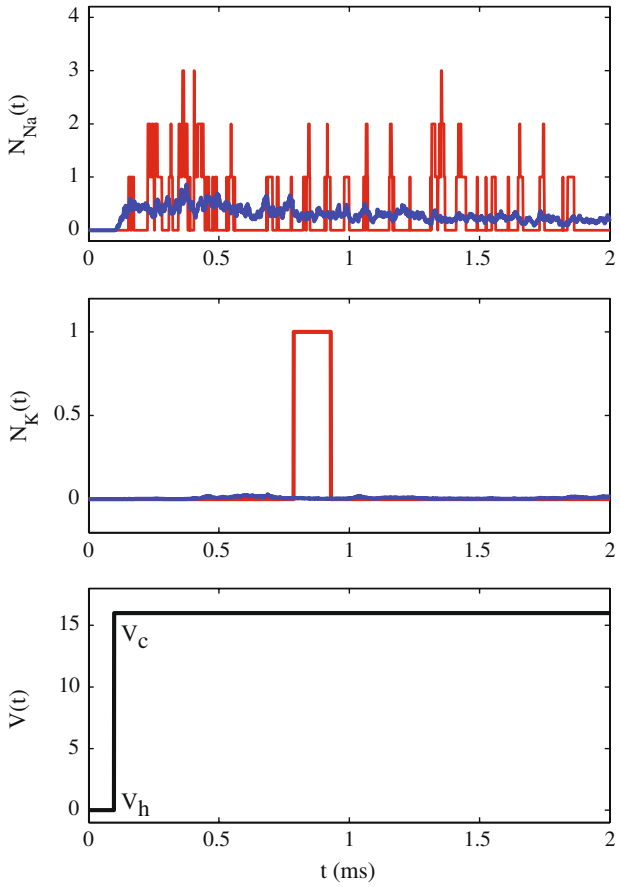

FIGURE 1. Example of voltage-step simulation results for a single trial. Top panel: Number of open sodium channels (out of 1000) at each time step for the Chow & White algorithm (red curve) and the Fox & Lu algorithm (blue curve) for the voltage step shown in the bottom panel. Middle panel: Number of open potassium channels (out of 333) at each time step. Bottom panel: Voltage step from V_h = 0 (resting potential) to V_c = 16 mV at time t = 0.1 ms.

the noise-term statistics analyses was 1 s, except for the results shown in Fig. 3 and in the top two panels of Fig. 7 in which a duration of 4 s was simulated. The number of sodium channels $N_{\mathrm{Na}}^{\max}$ was varied from 100 to 20,000, with the number of potassium channels $N_{\mathrm{K}}^{\max}$ always set to one third of the number of sodium channels (rounded to the nearest integer).

Simulations to analyze AP generation statistics were based on the membrane model of Mino *et al.*[25] and Bruce[2] but with the number of sodium channels $N_{\mathrm{Na}}^{\max}$ varied from 100 to 10,000. The membrane equation for this model is (Eq. 6 of Mino *et al.*[25])

$$C_m \frac{dV(t)}{dt} + \gamma_{\mathrm{Na}} \cdot \mathrm{nint}(N_{\mathrm{Na}}(t))[V(t) - E_{\mathrm{Na}}] + \frac{V(t)}{R_m} = I(t), \tag{24}$$

where C_m is the membrane capacitance, $V(t)$ is the relative transmembrane potential at time t, γ_{Na} (= 25.69 pS) is the single-channel sodium conductance, nint(·) indicates rounding to the nearest integer, $N_{\mathrm{Na}}(t)$ is the number of sodium channels open at time t, E_{Na} (= 144 mV) is the sodium equilibrium potential relative to the resting potential, and $I(t)$ is the stimulus current amplitude at time t. The results of Bruce[2] prompted the rounding of the number of open sodium channels to the nearest integer for the Fox & Lu algorithm. A potassium current was not included in the model, primarily to be consistent with the model of Mino *et al.*[25] and Bruce,[2] but also because the delayed-rectifier potassium current (described by Eqs. 2, 22, and 23) was found to have negligible effect on the threshold current statistics for the brief stimulating pulse.

In considering the effects of changing the number of sodium channels, two different cases are considered: constant channel density and constant membrane area. For a *constant channel density*, the area of the membrane patch is scaled proportionally to the number of sodium channels, as described by Rubinstein.[28] Based on the model's membrane capacitance and resistance for 1000 channels,[2] the membrane capacitance and resistance for $N_{\mathrm{Na}}^{\max}$ channels in this case are, respectively,

$$C_m = 0.0714 \times \frac{N_{\mathrm{Na}}^{\max}}{1000}\ \mathrm{pF} \quad \text{and} \quad R_m = 1953.49 \times \frac{1000}{N_{\mathrm{Na}}^{\max}}\ \mathrm{M\Omega}. \tag{25}$$

In the case of a *constant membrane area*, $C_m = 0.0714$ pF and $R_m = 1953.49$ MΩ, independent of $N_{\mathrm{Na}}^{\max}$, and consequently the channel density increases with increasing $N_{\mathrm{Na}}^{\max}$.

The stimulus for the AP analysis was a single 100-μs monophasic depolarizing current pulse, and at each stimulus current level the firing efficiency was calculated from 1000 repetitions of the stimulus. The membrane equation (Eq. 24) was solved using the Euler method with a time step of $\Delta t = 1$ μs, and the number of open channels at each time step was computed using an "exact" algorithm or the Fox & Lu algorithm as described above.

"Exact" algorithm results shown below were obtained with the Chow & White algorithm[9]; some simulations were also run using the Rubinstein algorithm[28] and were found to give similar results. Model code is available from the author on request.

RESULTS

Open Channel Statistics for a Voltage Step

Open channel statistics were analyzed for 1000 sodium and 333 potassium channels subject to a

voltage step. An example of the simulation results for a single current step from $V_h = 0$ (i.e., the resting potential) to $V_c = 16$ mV is given in Fig. 1. The number of open sodium channels for the Chow & White algorithm (red curve in top panel) is seen to be zero at the resting potential, and following the voltage step at time $t = 0.1$ ms the number of open channels flicks stochastically between integer values from zero to three channels. A greater frequency of two or three open sodium channels is seen early after the voltage step, as sodium activation quickly reaches its steady state, and then the frequency drops as sodium inactivation catches up. In contrast, the Fox & Lu algorithm (blue curve) exhibits a non-integer number of open sodium channels that follows the mean number of open channels from the Chow & White algorithm, with some small continuous stochastic fluctuations around the mean. The number of open potassium channels for the Chow & White algorithm (red curve in middle panel of Fig. 1) is seen to be zero most of the time for this voltage step, but one channel opens from time $t = 0.79$ ms to $t = 0.93$ ms in this trial. The number of open potassium channels for the Fox & Lu algorithm (red curve in middle panel) stays near zero in this trial, with some small continuous stochastic fluctuations.

Means and standard deviations of open channel numbers are shown in Fig. 2 for 1000 trials of three different voltage steps. The mean number of open sodium (left column) and potassium (right column) channels are seen to be nearly identical at each time step for the two algorithms. However, the standard deviations in the number of open channels, indicated by the error bars, are only similar for the two algorithms at the clamp potential of $V_c = 48$ mV (top row)—the Fox & Lu algorithm (blue curves and error bars) greatly underestimates the standard deviation in number of open channels for the Chow & White algorithm (red curves and error bars) for the clamp potentials of 24 and 16 mV (middle and bottom rows, respectively).

These observations motivate the analysis of the equivalent noise-term statistics required for the Fox & Lu algorithm to track the number of open channels in the Chow & White algorithm at each time step.

Equivalent Gating Particle Noise-Term Statistics

Figure 3 gives an analysis of the dynamics of the activation and inactivation particles at $V = 17$ mV. This value of the relative transmembrane potential was

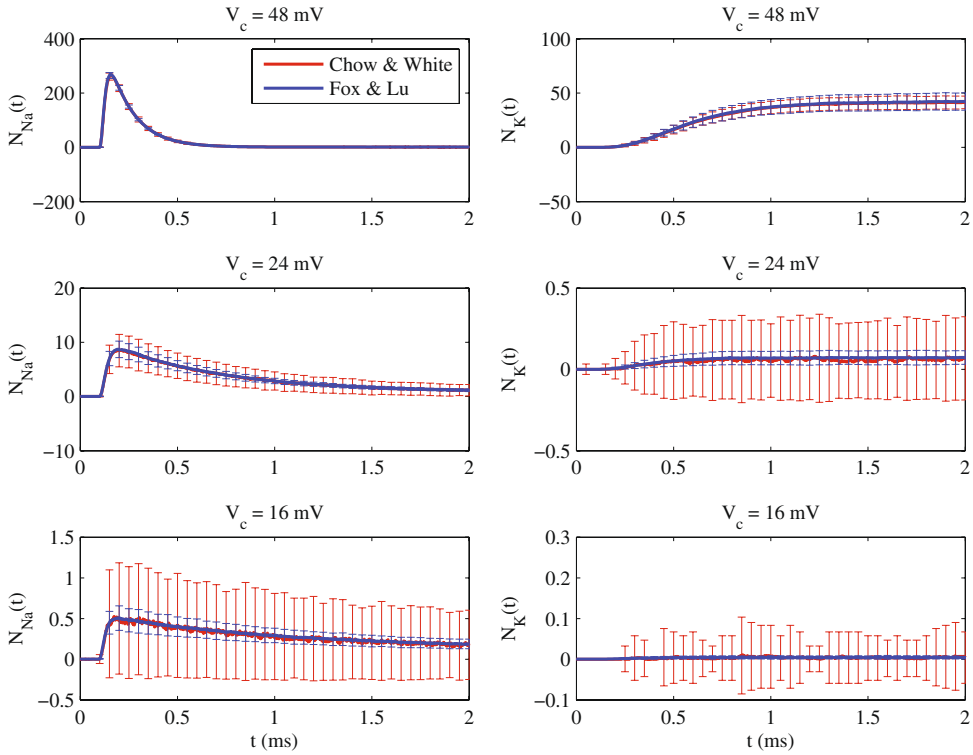

FIGURE 2. Mean and standard deviation in number of open channels as a function of time for 1000 trials. Statistics are shown for 1000 sodium channels (left column) and 333 potassium channels (right column) for voltage steps starting at the resting potential and stepping to 48 mV (top row), 24 mV (middle row), or 16 mV (bottom row). The curves show the mean for the Chow & White algorithm (red curve) and the Fox & Lu algorithm (blue curve) at every time step, and error bars indicate the standard deviations for every 50th time step.

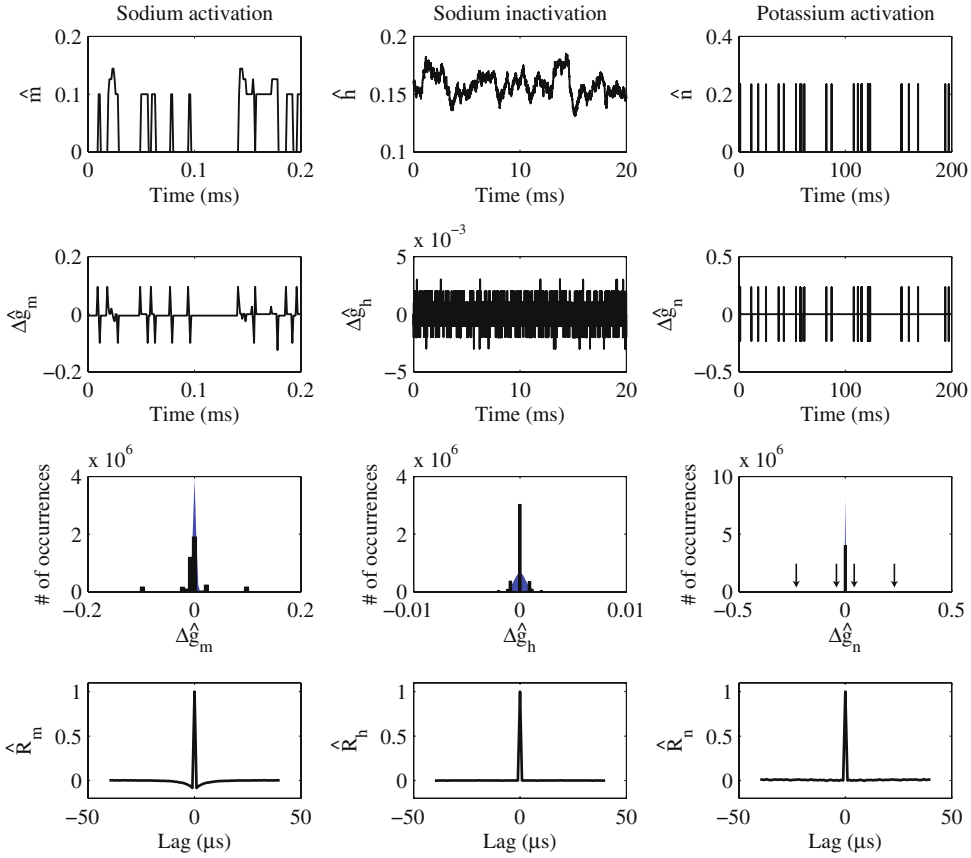

FIGURE 3. Activation (left column) and inactivation (middle column) dynamics of 1000 sodium channels and activation dynamics (right column) of 333 potassium channels at a relative transmembrane potential $V = 17$ mV. Top row: Example time series for $\hat{m}$, $\hat{h}$, and $\hat{n}$. Second row: Time series for noise terms $\Delta\hat{g}_m$, $\Delta\hat{g}_h$, and $\Delta\hat{g}_n$ corresponding to the particle time series from the top row. Third row: Histograms of values of $\Delta\hat{g}_m$, $\Delta\hat{g}_h$, and $\Delta\hat{g}_n$. The theoretical distributions derived by Fox and Lu[12,13] are shown by the blue-filled Gaussian curves. Bottom row: Autocorrelation functions for $\Delta\hat{g}_m$, $\Delta\hat{g}_h$, and $\Delta\hat{g}_n$.

chosen because the maximum inaccuracy in the Fox & Lu algorithm was found to occur around this membrane potential for sodium activation dynamics (see Fig. 4). Furthermore, this membrane potential is of interest because it is approximately 2/3 of the threshold potential in the model of Mino *et al.*[25] and Bruce,[2] and consequently the gating particle dynamics at this potential will have a substantial effect on the statistics of AP generation. In the left column of Fig. 3, the middle two panels show that at this transmembrane potential the Fox & Lu noise term required to match the *m*-particle dynamics from the Chow & White algorithm has small values near zero for most time steps but has infrequent large values in positive and negative pairs. These values are well outside the Gaussian distribution of values from the Fox & Lu algorithm. The autocorrelation function in the bottom left panel indicates that these large positive and negative values are correlated on a time scale of several microseconds, unlike the Fox & Lu noise term, which is uncorrelated. The example time series for $\hat{m}$ plotted in the top left panel shows that these correlated noise values correspond to brief openings or closings of small numbers of gating particles.

An analysis of the dynamics of sodium inactivation particles at $V = 17$ mV is given in the middle column of Fig. 3. The histogram of noise values shown in the third row of the middle column indicates that at this transmembrane potential the Fox & Lu noise term required to match the *h*-particle dynamics from the Chow & White algorithm has a distribution of finite values with a similar shape, mean and standard deviation to the Gaussian distribution of values from the Fox & Lu algorithm. The autocorrelation function in the bottom row of the middle column indicates that the estimated noise term for sodium inactivation particles is uncorrelated, like the Fox & Lu noise term.

The right column of Fig. 3 gives an analysis of the dynamics of potassium activation particles at $V = 17$ mV. The middle two panels show that at this transmembrane potential the Fox & Lu noise term required to match the *n*-particle dynamics from the

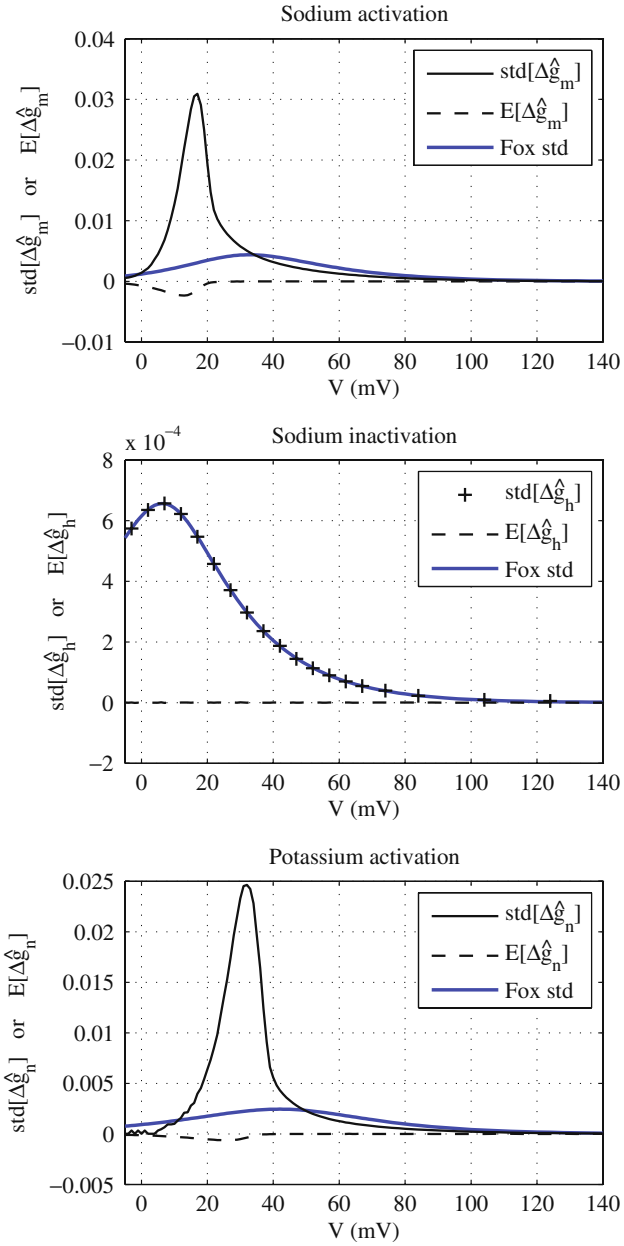

FIGURE 4. Effects of membrane potential on activation and inactivation noise term statistics. Top panel: standard deviation and mean of $\Delta\hat{g}_m$ as a function the relative transmembrane potential *V* for 1000 sodium channels. Middle panel: standard deviation and mean of $\Delta\hat{g}_h$ as a function the relative transmembrane potential *V* for 1000 sodium channels. Bottom panel: standard deviation and mean of $\Delta\hat{g}_n$ as a function the relative transmembrane potential *V* for 333 potassium channels. The theoretical standard deviation vs. membrane potential relationships given by Eq. (8) are shown in each panel for comparison.

Chow & White algorithm has very small values near zero for most time steps but has two pairs of very infrequent large positive and negative values indicated by the arrows. As was the case for sodium activation particles, these values for potassium are well outside the Gaussian distribution of values from the Fox & Lu algorithm. The autocorrelation function in the bottom right panel indicates that these large positive and negative values are correlated on a time scale of tens of microseconds. The example time series for $\hat{n}$ plotted in the top right panel shows that these correlated noise values correspond to brief openings of 1 out of the 333 potassium channels.

Shown in Fig. 4 are plots of the noise term time-series standard deviation and mean as a function of V for sodium activation, sodium inactivation, and potassium activation, respectively. The h-particle standard deviation curve (+) is close to the theoretical standard deviation curve (blue line) from the Fox & Lu algorithm (middle panel of Fig. 4). However, the m-particle and n-particle standard deviation curves (black solid lines in the top and bottom panels, respectively, of Fig. 4) are quite different from their corresponding theoretical standard deviation curves (blue lines); the peaks occur at a lower membrane potential than the theoretical curves, and they have substantially larger maxima.

The noise terms' time-series means are shown by the dashed lines in Fig. 4. Again, the h-particle curve (middle panel) matches the theoretical mean of zero from the Fox & Lu algorithm, whereas the m-particle and n-particle means (top and bottom panels, respectively, of Fig. 4) have appreciably large negative values in the region from the resting potential (0 mV) to the AP threshold potential (~24 mV) for the model of Mino *et al.*[25] and Bruce.[2]

Since the m-particle and n-particle noise term time series estimated from the Chow & White algorithm both exhibit correlations over time and these noise terms have an accumulative effect on the m-particle and n-particle values according to Eq. (11), it is of interest to determine the effective standard deviations of the noise terms accumulated over different time scales.

To do this, the standard deviations are calculated for values of $\Delta\hat{g}_m$, $\Delta\hat{g}_h$, and $\Delta\hat{g}_n$ integrated over contiguous time windows of duration T. If L is the total number of samples in a noise term sequence $\Delta\hat{g}_x$, $P = T/\Delta t$ is the number of samples in a time window of duration T, and $J = L/P$ is the number of contiguous integration windows, then the sequence

$$\bar{g}_x[j] = \sum_{p=0}^{P-1} \Delta\hat{g}_x[j \cdot P + p] \tag{26}$$

gives the accumulated noise term for each integration window $j = 0, 1, \ldots, J-1$. The normalized time-series standard deviation (i.e., the average standard deviation per simulation time step Δt over the integration

duration T) of the accumulated noise term sequence is then given by

$$\sigma_{\bar{g}_x} = \sqrt{\mathrm{var}[\bar{g}_x]/P}, \tag{27}$$

where var[·] is the time-series variance. For an uncorrelated noise-term sequence, such as the theoretical Fox & Lu noise-term sequences, the normalized standard deviation is independent of T.

Plotted in Fig. 5 are standard deviation curves for different values of T, as indicated on the plots. The standard deviation curves all begin to reach their respective asymptotic curves at an integration period of $T = 1$ ms, indicating that all the correlations in each noise term time series have been averaged out over this time period. The h-particle standard deviation curves all match the theoretical curve (middle panel of Fig. 5); the m-particle and n-particle standard deviation curve asymptotes have smaller maxima than their respective curves without integration (i.e., $T = 1$ ms) but do not match their respective theoretical curves (as indicated in the top and bottom panels of Fig. 5).

Similar temporal smoothing effects on the noise-term statistics are also observed if simulations are run with a Euler time step Δt larger than the 1 μs that is used in this manuscript (results not shown). However, the Euler approximation of the deterministic component of the gating particles' differential equations (Eq. 5) in the Fox & Lu algorithm would deteriorate for larger time steps.

Shown in Fig. 6, simulation results obtained for different numbers of sodium channels $N_{\mathrm{Na}}^{\max}$ and potassium channels $N_{\mathrm{K}}^{\max}$ were qualitatively similar to the results shown above for the standard number of channels. Just as the theoretical standard deviation scales with the reciprocal of the number of channels according to Eq. (7), the standard deviations estimated from the Chow & White algorithm also scale with the reciprocal of the number of channels. However, the empirical standard deviation curves for sodium and potassium activation in Fig. 6 do *not* converge towards their theoretical counterparts with increasing channel number; the inaccuracies of the Fox & Lu algorithm for channels with multiple activation particles per channel remain even for the largest numbers of channels investigated in this study.

From the results described above, it can be seen that the Fox & Lu algorithm provides a reasonable approximation of the single sodium channel inactivation particle h but not of the three sodium or four potassium activation particles m and n, respectively. To determine if the origin of the inaccuracies lies in the multiple activation particles per channel, some simulations were performed with a modified sodium channel incorporating just a single activation particle m

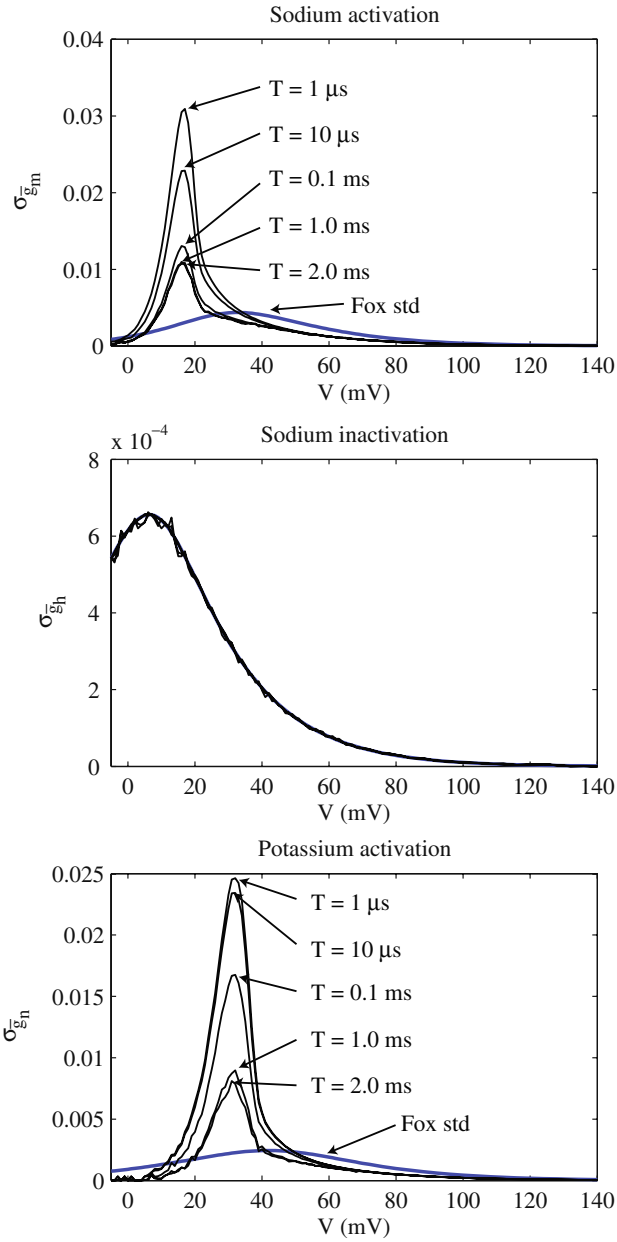

FIGURE 5. Effect of temporal integration on normalized standard deviations of noise terms as a function the relative transmembrane potential *V* for 1000 sodium channels and 333 potassium channels. Normalized standard deviations are calculated for values of $\Delta\hat{g}_m$ (top panel), $\Delta\hat{g}_h$ (middle panel), and $\Delta\hat{g}_n$ (bottom panel) averaged according to Eq. (27) over contiguous time windows of duration *T*, as indicated by the arrows. For comparison, the theoretical standard deviation vs. membrane potential relationships given by Eq. (8) are shown by the blue lines in each panel.

rather than the normal three particles. Markov kinetics for gating of this modified sodium channel are given by

$$\begin{array}{ccc} m_0h_0 & \underset{\beta_m}{\overset{\alpha_m}{\rightleftharpoons}} & m_1h_0 \\ \alpha_h\downarrow\uparrow\beta_h & & \alpha_h\downarrow\uparrow\beta_h. \\ m_0h_1 & \underset{\beta_m}{\overset{\alpha_m}{\rightleftharpoons}} & m_1h_1 \end{array} \tag{28}$$

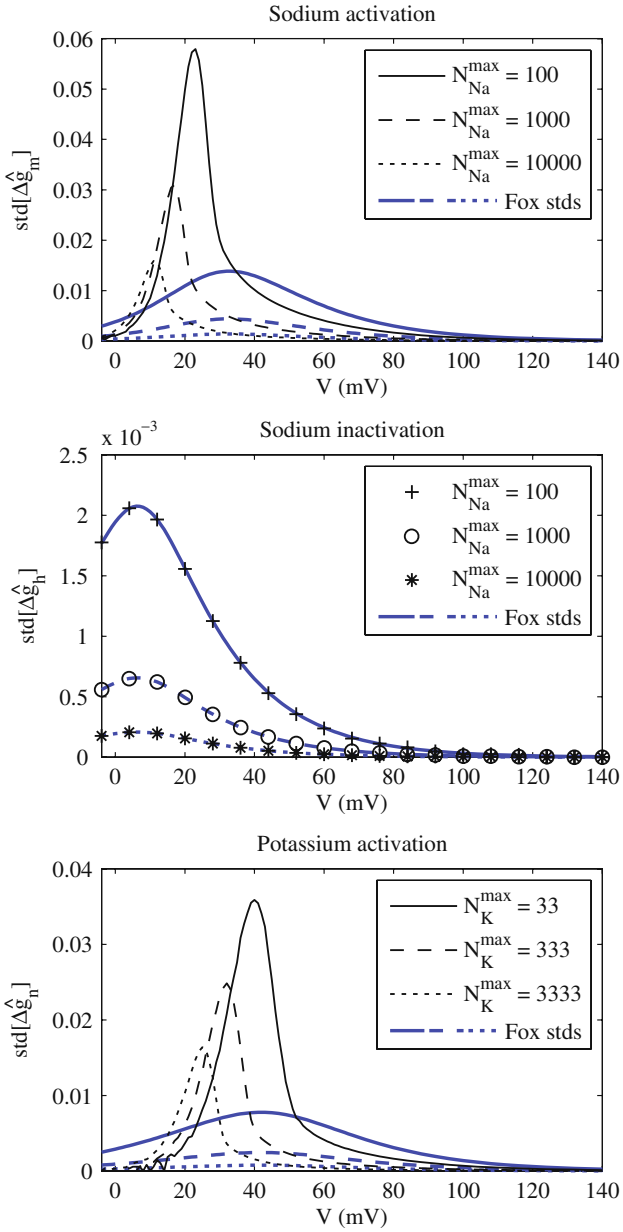

FIGURE 6. Effect of number of channels on standard deviations of $\Delta\hat{g}_m$ (top panel), $\Delta\hat{g}_h$ (middle panel), and $\Delta\hat{g}_n$ (bottom panel) as a function the relative transmembrane potential *V*. The theoretical standard deviation vs. membrane potential relationships given by Eq. (8) are shown in each panel for comparison.

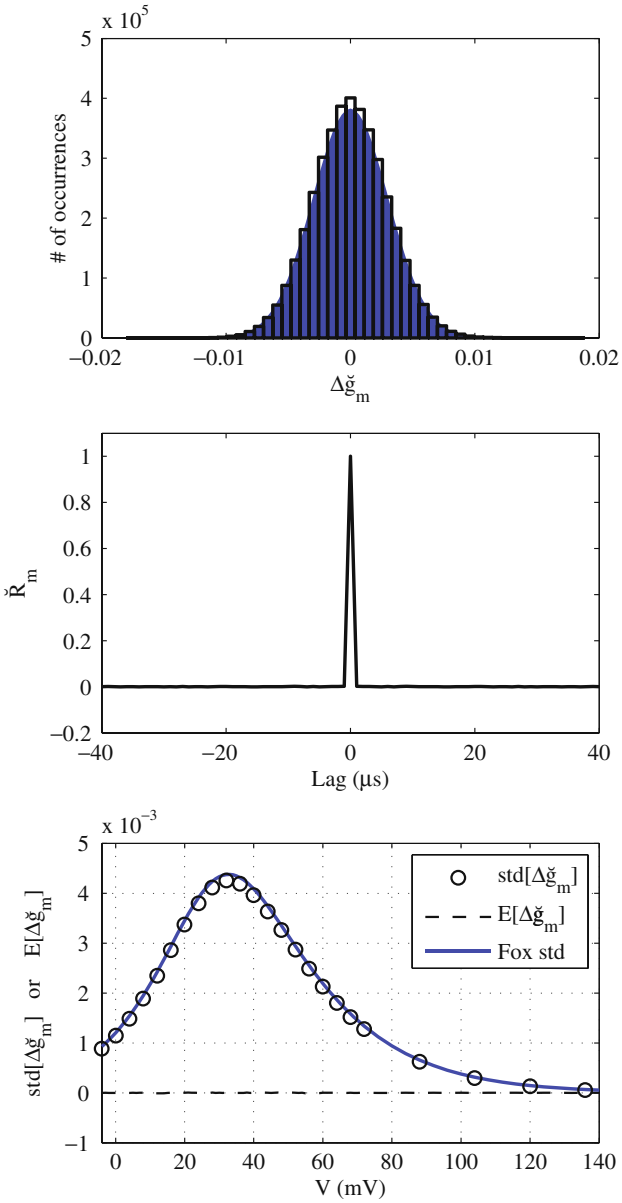

FIGURE 7. Modified *single m-particle* sodium channel model. Top panel: Histogram of values of noise term $\Delta\check{g}_m$ at a relative transmembrane potential $V = 17$ mV for 1000 sodium channels with single *m*-particles, modeled according to Eq. (28). The theoretical distribution derived by Fox and Lu[12,13] is shown by the blue-filled Gaussian curve. Middle panel: Autocorrelation function for $\Delta\check{g}_m$ at a relative transmembrane potential $V = 17$ mV for 1000 sodium channels with single *m*-particles. Bottom panel: standard deviation and mean of $\Delta\check{g}_m$ as a function the relative transmembrane potential *V* for 1000 sodium channels. The theoretical standard deviation vs. membrane potential relationship given by Eq. (8) is shown for comparison.

From Eq. (28), the fraction of sodium channels with an open *m* particle is

$$\check{m} = \frac{N_{m_1h_0} + N_{m_1h_1}}{N_{\mathrm{Na}}^{\max}}, \tag{29}$$

and the corresponding noise term estimated using Eq. (15) is $\Delta\check{g}_m$.

Figure 7 shows that, in contrast to the standard sodium channel model, the *m*-particle statistics for the single *m*-particle sodium channel are well described by the Fox & Lu algorithm. The top panel of Fig. 7 shows that the distribution of noise term values in the modified sodium channel model is well described by Fox

and Lu's theoretical distribution at a relative transmembrane potential $V = 17$ mV. This noise term is also uncorrelated at a relative transmembrane potential $V = 17$ mV (see the middle panel of Fig. 7), in agreement with Fox and Lu's derivation. In the bottom panel of Fig. 7, it can be seen that these results hold true over the entire range of transmembrane potentials. Consequently, it can be concluded that the problem with the Fox & Lu SDE formulation is that it does not capture the effect of small numbers of channels flicking briefly open or closed due to the combined action of multiple gating particles per channel.

Action Potential Statistics

In Fig. 8, mean threshold current (top row) and RS (bottom row) are plotted as a function N_{Na}^{max} for the constant channel density case (left column) and the constant membrane area case (right column). As was observed by Rubinstein for his "exact" Markov process algorithm,[28] RS drops as a function of increasing N_{Na}^{max} for both the Chow & White algorithm and the Fox & Lu algorithm in the case of a constant channel density. However, the curves for these two algorithms do *not* converge at high values of N_{Na}^{max}; rather, they maintain a ratio of around 2:1, such that they would only converge at RS = 0 as $N_{Na}^{max} \to \infty$.

In the case of a constant membrane area and channel density increasing with increasing N_{Na}^{max}, the threshold current (top right panel of Fig. 8) *decreases* slightly as a function of increasing N_{Na}^{max}, in contrast to the greatly increasing threshold current for the constant channel density simulation (top left panel). Along with this decreasing threshold current, RS is seen to decrease as a function of increasing N_{Na}^{max} for the Fox & Lu algorithm (bottom right panel of Fig. 8), whereas RS for the Chow & White drops slightly as N_{Na}^{max} is increased from 100 to 500 and then starts increasing again for $N \geq 1000$, such that the curves diverge rather than converge in the case of a constant membrane area.

The results of Fig. 7 indicate that the Fox & Lu approximation of gating kinetics is improved in the case of a modified sodium channel with just a single activation particle. To investigate the resultant effects on AP generation, simulations were run utilizing the modified sodium channel that has only a single stochastic m particle ($\breve{m}$) and a single stochastic h particle, as described by Eq. (28). However, in order to produce a threshold potential and AP temporal waveform similar to that of the standard sodium channel model, here the equations for the transition rates [$\alpha_m(V)$ and $\beta_m(V)$] are modified such that the steady-state activation ($\breve{m}_\infty$) vs. membrane potential curve of the single m particle matches that of the standard sodium channel (m_∞) cubed, i.e., $\breve{m}_\infty = \alpha_{\breve{m}}/(\alpha_{\breve{m}} + \beta_{\breve{m}}) = m_\infty^3$, while the time constant is unchanged, i.e., $\tau_{\breve{m}} = 1/(\alpha_{\breve{m}} + \beta_{\breve{m}}) = \tau_m$.

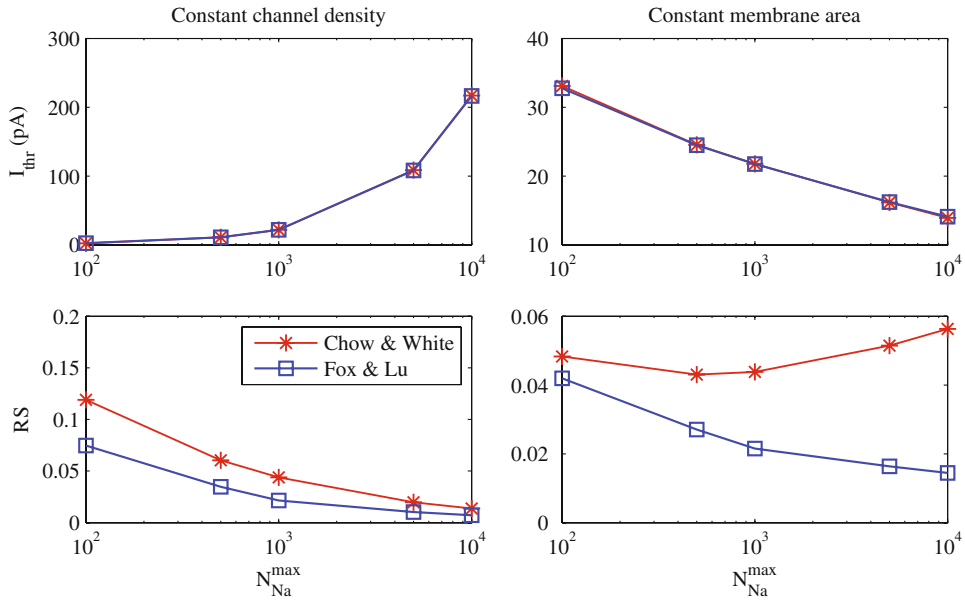

FIGURE 8. Action potential statistics as a function of the number of sodium channels for the standard sodium channel model. Left column: Constant channel density simulations; Right column: Constant membrane area simulations. Top row: Threshold current amplitude vs. number of sodium channels for the Chow & White (*) algorithm and the Fox & Lu algorithm (□). Bottom row: RS vs. number of sodium channels for the two algorithms.

The results for this single m-particle model are shown in the top panel of Fig. 9. Once again, the membrane capacitance and leakage resistance are scaled with $N_{\mathrm{Na}}^{\max}$ such that a constant channel density is maintained. In this case of a single stochastic m particle and a single stochastic h particle, the RS vs. $N_{\mathrm{Na}}^{\max}$ curves for the Chow & White and Fox & Lu algorithms now converge for $N \geq 5000$.

While the RS value is determined primarily by the statistics of sodium activation, the h particle does have a small influence. Consequently, another set of simulations was run with a model having a single stochastic m particle (as described above) and a single *deterministic* h particle. For the Fox & Lu algorithm, this is achieved by utilizing the Hodgkin–Huxley deterministic ODE for the h particle dynamics (equivalent to setting the Fox & Lu noise-term standard deviation to zero). For the Chow & White algorithm, the m particle is modeled by the Markov process $m_0 \underset{\beta_m}{\overset{\alpha_m}{\rightleftharpoons}} m_1$, the h particle is modeled by the HH deterministic ODE, and the number of open sodium channels is given by $\mathrm{nint}(N_{m_1} \cdot h)$. The results for this model, given in the bottom panel of Fig. 9, show that with the deterministic h particle and single stochastic m particle the RS vs. $N_{\mathrm{Na}}^{\max}$ curves for the Chow & White and Fox & Lu algorithms now converge for $N \geq 1000$.

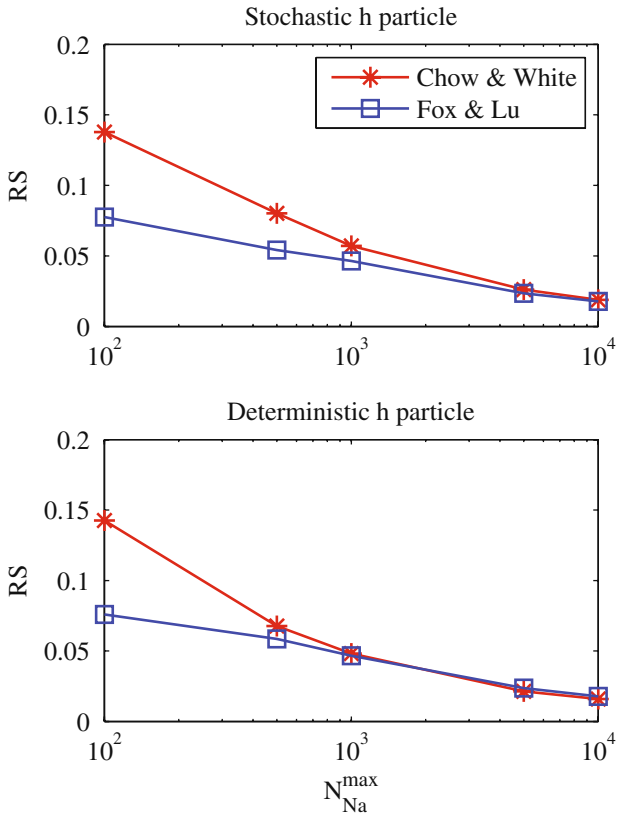

FIGURE 9. Relative spread as a function of the number of sodium channels for single stochastic *m*-particle model, with a single stochastic *h* particle (top panel) or a single deterministic *h* particle (bottom panel), for the Chow & White (*) algorithm and the Fox & Lu algorithm (□).

It is also of interest to determine whether the results shown in Figs. 4 and 5 are sufficient to explain the magnitude of the difference in RS values for the standard sodium channel model with $N_{\mathrm{Na}}^{\max} = 1000$, i.e., the model studied in Mino *et al.*[25] and Bruce.[2] For this number of channels, RS values obtained with the Chow & White algorithm are around two times larger than those produced by the Fox & Lu algorithm in the case of stimulation by a 100-μs depolarizing current pulse. At the membrane's threshold potential of $V \approx 24$ mV, the Fox & Lu theoretical noise term standard deviation is 0.0039 for each 1 μs time step, whereas the empirical noise term standard deviation per time step is just over twice this at a value 0.0093. However, at 16–17 mV the empirical standard deviation is more than ten times the theoretical value (see Fig. 4). Consequently, these ratios cannot directly explain the two-to-one ratio of RS values for the two algorithms; the accumulated effects of the noise term must be taken into account, since the correlations in the noise term reduce the effective standard deviation over longer time periods (see Fig. 5).

To test out the effective noise-term integration period for this particular model and stimulus, some simulations were run with an *ad hoc* modification of the Fox & Lu algorithm. In these simulations, uncorrelated Gaussian noise terms were used, but instead of using the theoretical standard deviation and mean vs. membrane potential relationships of Fox and Lu (Eqs. 6 and 8), fits to the empirical standard deviation and mean vs. membrane potential relationships (shown in Figs. 4 and 5 above) for different noise-term integration time periods were used for the m particles. It was found that for a noise-term integration period of 60–80 μs the modified Fox & Lu model produced RS values very close to that of the Chow & White algorithm.

Figure 10 shows FE vs. current amplitude curves for the Chow & White algorithm (*), the Fox & Lu algorithm with the theoretically derived noise term statistics (□) and the modified Fox & Lu algorithm (+) utilizing empirically derived noise-term mean and standard deviation functions for an integration period of $T = 64$ μs. This noise-term integration period is reasonable given that for a 100-μs, marginally subthreshold current pulse the membrane potential is within a few millivolt of the threshold potential for approximately this period of time. The Chow & White algorithm for this stimulus has a mean threshold current I_{thr} of 21.77 pA and RS = 0.0438 with $N_{\mathrm{Na}}^{\max} = 1000$. The threshold and RS values for the Fox & Lu

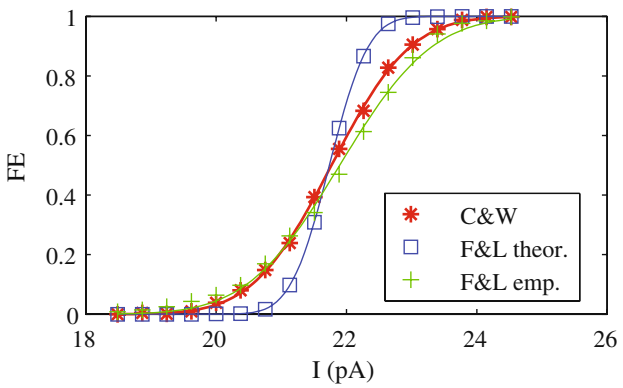

FIGURE 10. Firing efficiency vs. stimulus current for the Chow & White (*) algorithm, the Fox & Lu algorithm with theoretical noise-term mean and standard deviation (□), and the Fox & Lu algorithm with empirically derived noise-term mean and standard deviation (+) as described in the text.

algorithm using the theoretical noise-term statistics (Eqs. 6 and 8) are 21.74 pA and 0.0215, respectively. For the "corrected" Fox & Lu algorithm, $I_{thr} = 21.90$ pA and RS = 0.0509. Thus, the threshold and RS values for the corrected Fox & Lu algorithm exceed those of the Chow & White algorithm only very slightly, which is a substantial improvement over the 2:1 ratio of RS values that the Chow & White and original Fox & Lu algorithms produce.

Such *ad hoc* correction of the Fox & Lu algorithm is possible when the stimulating pulse duration is fixed, but unfortunately it is somewhat cumbersome to apply for cases where the pulse duration varies and it is not easily generalizable to arbitrary stimuli.

DISCUSSION

The results of this study have important implications for the interpretation of investigations reported in the literature using the Fox & Lu method.[7,8,10,14,15,19,26,27,31–39,45,47–49] First, predictions of membrane dynamics and response properties that are dependent on the statistics of ion channel gating are likely to be at least somewhat inaccurate using the Fox & Lu algorithm for channels with multiple stochastic gating particles, as was originally observed in Mino *et al.*[25] and Bruce.[2] Second, it cannot be assumed that simply having a large number of ion channels will make the Fox & Lu approximation valid (see Figs. 6 and 8) in channels with multiple stochastic gating particles.

Several of the published studies[38,39,48,49] did include comparisons of results obtained utilizing the Fox & Lu approximation and an "exact" method while varying the number of ion channels. Shuai and Jung[38] examined the effects of incorporating stochastic gating of the *three* slow-inactivation particles of inositol 1,4,5-triphosphate (IP_3) receptor channels in a model of pancreatic β cells. In Fig. 3 of Shuai and Jung,[38] the results for the Langevin and Markov models have not converged for $N = 1000$, although from extrapolation of the curves it appears convergence might occur for much larger values of N. In Fig. 4(a) of Shuai and Jung,[38] the results converge for large N, but they converge to a calcium concentration variance of zero, i.e., the stochastic behavior is becoming negligible. In another study,[39] they investigated the effects of clustering of voltage-gated sodium channels in a one-dimensional cable model of an axon or an active dendrite. The statistics of spontaneous AP generation were similar for the two methods for larger cluster sizes but not for smaller cluster sizes, as shown in Figs. 2, 4, and 10 of Shuai and Jung.[39] However, the Langevin description is used only for a *single* inactivation particle in this model, and sodium activation is modeled as instantaneous and deterministic (see Eq. 22 of Shuai and Jung[39]). Zeng and Jung[48] studied the statistics of interspike intervals produced by a Hodgkin–Huxley model with stochastic sodium and potassium channels as a function of membrane area for a fixed channel density, i.e., as a function of number of ion channels. In Fig. 4 of Zeng and Jung,[48] the average interspike intervals for the Fox & Lu method and a Markov process method *diverge* with increasing membrane area above ~0.8 μm^2, corresponding to $N_{Na}^{max} > 48$ and $N_K^{max} > 16$ for the channel densities used. Zhan and colleagues[49] investigated a model of a calcium channel with *three* slow inactivation particles similar to that of Shuai and Jung.[38] Comparisons of the Langevin and Markov methods are made in Figs. 6 and 7 of Zhan *et al.*[49] Comparing panels H1 and H2 of Fig. 6 of Zhan *et al.*,[49] which are the Langevin and Markov results, respectively, for the largest number of channels [$N = 20{,}000$], the curves are clearly different. A visual comparison is harder to make in Fig. 7 of Zhan *et al.*,[49] but it appears that the results in panels H1 and H2 are also somewhat different. Consequently, the results of the published comparisons appear consistent with the conclusions of this present study: in contrast to the convergence observed in channels with a single stochastic gating particle,[39,42] increased accuracy of the Fox & Lu algorithm for larger numbers of ion channels is not always observed in models with multiple stochastic gating particles per channel. Furthermore, as was observed by Zeng and Jung,[48] it appears that in some cases the accuracy of the Fox & Lu approximation may *worsen* with increasing numbers of channels. This was found in the present study for predictions of RS in the case of increasing channel numbers in a patch of membrane

with constant area (see the bottom right panel of Fig. 8).

In Fox and Lu's derivations, an intermediate Langevin description does include the coupling of the states of the multiple gating particles in an ion channel (see Eqs. 33–36 of Fox and Lu[13] or Eqs. 11–16 and 22–27 of Fox[12]). However, solution of the intermediate model requires computation of a matrix square root at each time step, reducing the computation speed substantially.[12] Consequently, the benefits of the final Langevin approximation over the Chow & White algorithm in terms of speed and simplicity are not shared with the intermediate model. In addition, the intermediate description does not facilitate the direct comparison with the deterministic Hodgkin–Huxley gating particle equations (and the resulting intuitive interpretation) that is provided by the final Langevin approximation.

Given the difficultly in determining in advance whether the Fox & Lu approximation is accurate enough for a given simulation, it would be advantageous to derive an analytical expression for the error in the Fox & Lu approximation.[12,13] It would appear from the results of this study that attempts to derive an analytical error metric should focus on the difference between the intermediate Langevin description and the final approximation, to capture the effect of "decoupling" the gating particle states in the final approximation.

ACKNOWLEDGMENTS

The author thanks Faheem Dinath and Melissa Perri for computer programming assistance and two anonymous reviewers for helpful comments on earlier versions of the manuscript. This work was supported by the Barber–Gennum Chair Endowment.

REFERENCES

[1]Bruce, I. C., Evaluation of approximate stochastic Hodgkin–Huxley models. In: Proceedings of 3rd International IEEE EMBS Conference on Neural Engineering. Piscataway, NJ: IEEE, 2007, pp. 654–658.

[2]Bruce, I. C. Implementation issues in approximate methods for stochastic Hodgkin–Huxley models. *Ann. Biomed. Eng*. 35:315–318, 2007.

[3]Bruce, I. C., and F. Dinath, Improved approximation of stochastic ion channel gating. In: Abstracts of the 9th International Conference on Cochlear Implants and Related Sciences (CI-2006), Vienna, Austria, 2006, pp. 87–88.

[4]Bruce, I. C., L. S. Irlicht, M. W. White, S. J. O'Leary, S. Dynes, E. Javel, and G. M. Clark. A stochastic model of the electrically stimulated auditory nerve: pulse-train response. *IEEE Trans. Biomed. Eng*. 46:630–637, 1999.

[5]Bruce, I. C., M. W. White, L. S. Irlicht, S. J. O'Leary, and G. M. Clark. The effects of stochastic neural activity in a model predicting intensity perception with cochlear implants: low-rate stimulation. *IEEE Trans. Biomed. Eng*. 46:1393–1404, 1999.

[6]Bruce, I. C., M. W. White, L. S. Irlicht, S. J. O'Leary, S. Dynes, E. Javel, and G. M. Clark. A stochastic model of the electrically stimulated auditory nerve: single-pulse response. *IEEE Trans. Biomed. Eng*. 46:617–629, 1999.

[7]Casado, J. M. Synchronization of two Hodgkin–Huxley neurons due to internal noise. *Phys. Lett. A* 310:400–406, 2003.

[8]Casado, J. M., and J. P. Baltanás. Phase switching in a system of two noisy Hodgkin–Huxley neurons coupled by a diffusive interaction. *Phys. Rev. E* 68:061917-1–061917-10, 2003.

[9]Chow, C. C., and J. A. White. Spontaneous action potentials due to channel fluctuations. *Biophys. J*. 71:3013–3021, 1996.

[10]de Vries, G., and A. Sherman. Channel sharing in pancreatic β-cells revisited: enhancement of emergent bursting by noise. *J. Theor. Biol*. 207:513–530, 2000.

[11]Ferguson, W. D., L. M. Collins, and D. W. Smith. Psychophysical threshold variability in cochlear implant subjects. *Hear. Res*. 180:101–113, 2003.

[12]Fox, R. F. Stochastic versions of the Hodgkin–Huxley equations. *Biophys. J*. 72:2068–2074, 1997.

[13]Fox, R. F., and Y.-N. Lu. Emergent collective behavior in large numbers of globally coupled independently stochastic ion channels. *Phys. Rev. E* 49:3421–3431, 1994.

[14]Gong, Y. B., M. S. Wang, Z. H. Hou, and H. W. Xin. Optimal spike coherence and synchronization on complex Hodgkin–Huxley neuron networks. *ChemPhysChem* 6:1042–1047, 2005.

[15]Güler, M. Dissipative stochastic mechanics for capturing neuronal dynamics under the influence of ion channel noise: formalism using a special membrane. *Phys. Rev. E* 76:041918-1–041918-17, 2007.

[16]Hodgkin, A., and A. Huxley. A quantitative description of membrane current and its application to conduction and excitation in nerve. *J. Physiol*. 117:500–544, 1952.

[17]Hong, R. S., and J. T. Rubinstein. High-rate conditioning pulse trains in cochlear implants: dynamic range measures with sinusoidal stimuli. *J. Acoust. Soc. Am*. 114:3327–3342, 2003.

[18]Hong, R. S., and J. T. Rubinstein. Conditioning pulse trains in cochlear implants: effects on loudness growth. *Otol. Neurotol*. 27:50–56, 2006.

[19]Jo, J., H. Kang, M. Y. Choi, and D.-S. Koh. How noise and coupling induce bursting action potentials in pancreatic β-cells. *Biophys. J*. 89:1534–1542, 2005.

[20]Krogh-Madsen, T., L. Glass, E. J. Doedel, and M. R. Guevara. Apparent discontinuities in the phase-resetting response of cardiac pacemakers. *J. Theor. Biol*. 230:499–519, 2004.

[21]Lerma, C., T. Krogh-Madsen, M. Guevara, and L. Glass. Stochastic aspects of cardiac arrhythmias. *J. Stat. Phys*. 128:347–374, 2007.

[22]Matsuoka, A. J., J. T. Rubinstein, P. J. Abbas, and C. A. Miller. The effects of interpulse interval on stochastic properties of electrical stimulation: models and measurements. *IEEE Trans. Biomed. Eng*. 48:416–424, 2001.

[23]Mino, H., and J. T. Rubinstein. Effects of neural refractoriness on spatio-temporal variability in spike initiations with electrical stimulation. *IEEE Trans. Neural Syst. Rehabil. Eng*. 14:273–280, 2006.
[24]Mino, H., J. T. Rubinstein, C. A. Miller, and P. J. Abbas. Effects of electrode-to-fiber distance on temporal neural response with electrical stimulation. *IEEE Trans. Biomed. Eng*. 51:13–20, 2004.
[25]Mino, H., J. T. Rubinstein, and J. A. White. Comparison of algorithms for the simulation of action potentials with stochastic sodium channels. *Ann. Biomed. Eng*. 30:578–587, 2002.
[26]Ozer, M., and N. H. Ekmekci. Effect of channel noise on the time-course of recovery from inactivation of sodium channels. *Phys. Lett. A* 338:150–154, 2005.
[27]Rowat, P. F., and R. C. Elson. State-dependent effects of Na channel noise on neuronal burst generation. *J. Comput. Neurosci*. 16:87–112, 2004.
[28]Rubinstein, J. T. Threshold fluctuations in an *N* sodium channel model of the node of Ranvier. *Biophys. J*. 68:779–785, 1995.
[29]Rubinstein, J. T., B. S. Wilson, C. C. Finley, and P. J. Abbas. Pseudospontaneous activity: stochastic independence of auditory nerve fibers with electrical stimulation. *Hear. Res*. 127:108–118, 1999.
[30]Runge-Samuelson, C. L., P. J. Abbas, J. T. Rubinstein, C. A. Miller, and B. K. Robinson. Response of the auditory nerve to sinusoidal electrical stimulation: effects of high-rate pulse trains. *Hear. Res*. 194:1–13, 2004.
[31]Sato, D., Y. Shiferaw, A. Garfinkel, J. N. Weiss, Z. Qu, and A. Karma. Spatially discordant alternans in cardiac tissue: role of calcium cycling. *Circ. Res*. 99:520–527, 2006.
[32]Schmid, G., I. Goychuk, and P. Hänggi. Stochastic resonance as a collective property of ion channel assemblies. *Europhys. Lett*. 56:22–28, 2001.
[33]Schmid, G., I. Goychuk, and P. Hänggi. Channel noise and synchronization in excitable membranes. *Physica A* 325:165–175, 2003.
[34]Schmid, G., I. Goychuk, and P. Hänggi. Controlling the spiking activity in excitable membranes via poisoning. *Physica A* 344:665–670, 2004.
[35]Schmid, G., I. Goychuk, and P. Hänggi. Effect of channel block on the spiking activity of excitable membranes in a stochastic Hodgkin–Huxley model. *Phys. Biol*. 1:61–66, 2004.
[36]Schmid, G., I. Goychuk, and P. Hänggi. Capacitance fluctuations causing channel noise reduction in stochastic Hodgkin–Huxley systems. *Phys. Biol*. 3:248–254, 2006.
[37]Schmid, G., and P. Hänggi. Intrinsic coherence resonance in excitable membrane patches. *Math. Biosci*. 207:235–245, 2007.
[38]Shuai, J. W., and P. Jung. Optimal intracellular calcium signaling. *Phys. Rev. Lett*. 88:068102-1–068102-4, 2002.
[39]Shuai, J. W., and P. Jung. The dynamics of small excitable ion channel clusters. *Chaos* 16:026104-1–026104-110, 2006.
[40]Strassberg, A. F., and L. J. DeFelice. Limitations of the Hodgkin–Huxley formalism: effects of single channel kinetics on transmembrane voltage dynamics. *Neural Comput*. 5:843–855, 1993.
[41]Tanskanen, A. J., J. L. Greenstein, B. O'Rourke, and R. L. Winslow. The role of stochastic and modal gating of cardiac L-type Ca^{2+} channels on early after-depolarizations. *Biophys. J*. 88:85–95, 2005.
[42]Tuckwell, H. C. Diffusion approximations to channel noise. *J. Theor. Biol*. 127:427–438, 1987.
[43]Tuckwell, H. C., and P. Lansky. On the simulation of biological diffusion processes. *Comput. Biol. Med*. 27:1–7, 1997.
[44]Verveen, A. A., and H. E. Derksen. Fluctuation phenomena in nerve membrane. *Proc. IEEE* 56:906–916, 1968.
[45]Wang, M. S., Z. H. Hou, and H. W. Xin. Double-system-size resonance for spiking activity of coupled Hodgkin–Huxley neurons. *ChemPhysChem* 5:1602–1605, 2004.
[46]White, J. A., J. T. Rubinstein, and A. R. Kay. Channel noise in neurons. *Trends Neurosci*. 23:131–137, 2000.
[47]Wu, D., Y. Jia, L. J. Yang, Q. Liu, and X. Zhan. Phase synchronization and coherence resonance of stochastic calcium oscillations in coupled hepatocytes. *Biophys. Chem*. 115:37–47, 2005.
[48]Zeng, S., and P. Jung. Mechanism for neuronal spike generation by small and large ion channel clusters. *Phys. Rev. E* 70:011903-1–011903-8, 2004.
[49]Zhan, X., D. Wu, L. Yang, Q. Liu, and Y. Jia. Effects of both glucose and IP_3 concentrations on action potentials in pancreatic β-cells. *Eur. Biophys. J*. 36:187–197, 2007.